RSC Advances

ROYAL SOCIETY OF CHEMISTRY

www.rsc.org/advances

2015/04/13

Submitted to *RSC Adv.*

Spin-Orbit Coupling Analyses on Phosphorescent Processes in $Ir(Zppy)_3$ (Z = NH_2, NO_2 and CN)

Shiro Koseki,[*ab] Harunobu Yoshinaga,[a] Toshio Asada[ab] and Takeshi Matsushita[bc]

[a]*Department of Chemistry, Graduate School of Science, Osaka Prefecture University, 1-1 Gakuen-cho, Sakai, Osaka 599-8531, Japan*

[b]*The Research Institute for Molecular Electronic Devices (RIMED), Osaka Prefecture University, 1-1 Gakuen-cho, Naka-ku, Sakai 599-8531, Japan*

[c]*JNC Petrochemical Corporation, 5-1 Goikaigan, Ichihara, Chiba 290-8551, Japan*

[*]E-mail: shiro@c.s.osakafu-u.ac.jp

†Electronic supplementary information (ESI) available. See DOI: 10.1039/###

ABSTRACT

Substituent effects of NH_2, NO_2 and CN groups to phosphorescence in *fac*-tris(2-phenylpyridinato)iridium(III) [*fac*-Ir(ppy)$_3$] were examined theoretically by using the multiconfiguration self-consistent field (MCSCF) method together with the SBKJC basis sets augmented by a set of polarization functions, followed by second-order configuration interaction (SOCI) and spin-orbit coupling (SOC) calculations, while time-dependent density functional theory (TD DFT) calculations provided too long wavelengths for phosphorescent peaks at the geometries optimized for triplet states even though the TD DFT predictions were qualitatively good with respect to relative spectral shifts. The strongest electron-donating substituent NH_2 and the strongest electron-withdrawing substituents, NO_2 and CN, were chosen for investigation of the substituent effects in the present investigation. It was found that when these electron-withdrawing substituents are introduced into the Z_5 sites, the largest blue shift is obtained for the emission spectra, while the introduction of electron-donating NH_2 substituent causes a red shift of emission spectra. This is because the Z_5 site has non-negligible coefficients in the highest occupied molecular orbital (HOMO) and can interact with the π^* orbitals of the substituents. This interaction makes the HOMO lower in energy. This is the reason why a large blue shift of the emission peak is obtained when one of these substituents is introduced to the Z_5 sites. Based on the results of calculation, it can be said that the best material for blue-color emission is tris(5-nitro-2-phenylpyridinato) iridium(III) [*fac*-Ir(5-NO_2ppy)$_3$] or tris(5-nitro-4,6-difluoro-2-phenylpyridinato)iridium(III) [*fac*-Ir(5-NO_2-4,6-dfppy)$_3$]. If the reactivity of the NO_2 substituent in the lowest triplet state becomes troublesome in synthesis processes and/or if it is difficult to choose host molecules for an emissive layer, tris(5-cyano-3,4,6-trifluoro-2-phenylpyridinato)iridium(III) [*fac*-Ir(5-CN-3,4,6-tfppy)$_3$] would be the most appropriate for blue-color emission.

1 Introduction

After highly luminescent organic molecules was proposed by Tang *et al.* of in 1989[1], research interest of theoretical chemists has been focused especially on elucidation of the electronic and photophysical features of phosphorescent organo-platinum and organo-iridium compounds. It is known that phosphorescence can be used, instead of fluorescence, to design more efficient organic light-emitting diodes (OLEDs). There are many theoretical reports, as well as experimental reports, on such OLEDs[2–40]. In most of the theoretical investigations, density functional theory (DFT) was used and the energies of the highest occupied molecular orbital (HOMO) and the lowest unoccupied molecular orbital (LUMO) in organo-metallic complexes were examined to estimate the emission energies or the wavelengths of fluorescence and phosphorescence. For a more reliable investigation based on theoretical calculations, Minaev *et al.*[29–40] used quadratic response (QR) approximation together with time-dependent (TD) DFT methods for estimating the lifetimes of phosphorescent states in various iridium complexes[29–40]. They reported excellent results for the lifetimes of phosphorescence in various iridium complexes.

In our research group[41–57], multi-configuration self-consistent field (MCSCF) wave functions[58] followed by second-order configuration interaction (SOCI) calculations[59] were used for explicitly calculating spin-orbit coupling (SOC) integrals, in which the Breit-Pauli (BP) Hamiltonian is employed, in order to describe low-lying electronic states in molecules including heavy atoms, while we found that TD DFT calculations provided too long wavelengths for phosphorescent peaks at the geometries optimized for triplet states, even though the TD DFT predictions were qualitatively good with respect to relative spectral shifts. In order to avoid computational difficulties and/or time-consuming calculations in such investigations, relativistic effective-core potentials (RECPs) or model-core potentials (MCPs) and their associated basis sets need to be employed. Although MCPs have correct orbital-nodes, they are not so popular unfortunately and have less variety of selections. On the other hand, RECPs have become very popular, especially in the research fields of heavy-metal complexes, and the use of RECPs provides many merits for theoretical investigation.

When RECPs are employed for SOC calculations, the full BP Hamiltonian provides very small SOC integrals because of node-less RECP orbitals. Therefore, it is necessary to introduce effective nuclear charges (Z_{eff})[41–47] for reasonable prediction of SOC effects. This is usually referred to as one-electron approximation, effective nuclear charge approximation, or Z_{eff} approximation. Our research group determined Z_{eff}'s for all transition elements and reported that this approximation works very well for estimation of SOC effects in mono-hydrides of transition elements in the third through seventh groups[48–50]. The di-hydrides and tetra-hydrides of rhenium atoms were also examined in our laboratory[51–54]. After such successes, this method was applied to theoretical investigations of the phosphorescent processes in OLED molecules[55–57]. The results of our

investigations could explain the emission spectra in the parent molecules, bis[2-(2'-thienyl) pyridinato]platinum [$Pt(thpy)_2$][55] and tris(2-phenylpyridinato)iridium(III) [$Ir(ppy)_3$].[56]. We also analyzed the geometrical effects of ligands in $Ir(ppy)_3$ and its derivatives.[57] In this latest paper, we discussed the effects of introducing an auxiliary ligand, picolinate (pic) or 2,4-pentanedionate (acac) ligand, to spectral shifts of phosphorescence. When such an auxiliary ligand is introduced, an iridium complex has not only *facial* (*fac*) and *meridional* (*mer*) isomers but also additional geometrical isomers. For example, the introduction of a pic ligand provides bis[2-(4',6'-difluorophenyl) pyridinato-N,C2'] [picolinato-N,O]iridium(III) [$Ir(4,6\text{-}dfppy)_2(pic)$], so-called **FIrpic**, and this complex has four geometrical isomers, homo-*N*-*trans* (HNT), homo-*C*-*trans* (HCT), homo-*cis*,hetero-N-*cis* (HC), and homo-*cis*,hetero-N-*trans* (HT) (see the details in ref.57). The alignment of the heaviest atoms in each ligand of HC is the same as *fac*-$Ir(ppy)_3$, but the most stable isomer is not HC but HNT among these four isomers. The calculated peak of the phosphorescence appears at the wavelength of 450 nm in HNT. Although this wavelength is shorter than the corresponding observed wavelengths (468–469 nm) by about 20 nm, this series of calculations indicate that a systematic underestimation is obtained for the peak wavelengths of emission because of inadequate consideration of electron correlation effects and that the magnitudes of spectral shifts are reliable for quantitative prediction of emission peaks. The next most stable isomer, HC, is only 0.8 (DFT) or 0.9 (MCSCF+SOCI+SOC) kcal/mol higher than HNT and is calculated to have a phosphorescent peak at the wavelength of 412 nm. Therefore, if only the HC isomer of **FIrpic** can be doped into an emissive layer of OLEDs, more blue-shifted phosphorescence is expected to be observed. In this investigation, we also discussed the phosphorescent processes in bis[2-(4',6'-difluorophenyl) pyridinato-N,C2'] [2,4-pentanedionato-O,O]iridium(III) [$Ir(4,6\text{-}dfppy)_2(acac)$], so-called **FIracac** and the related complexes.[57]

Although large amount of investigations have been reported so far on OLED materials, it is still expected that better materials need to be developed for brighter blue phosphorescence. Therefore, we think it is valuable to theoretically examine the effects of strongest electro-donating substitutent NH_2 and strongest electro-withdrawing substituents, CN and NO_2, since we could not find any information on the substituent effects of NH_2 and NO_2 groups. The methods of theoretical calculation are described in detail in the next section. In the third section, the effects of NH_2, NO_2, and CN substituents on the phenyl rings of ppy ligands are compared and discussed, where NH_2 group should be considered to be a representative for some bulky NX_2 groups (X could be alkyl, aryl or any other functional group). Finally, better phosphorescent complexes for brighter blue-color emission are suggested on the basis of the present discussion on iridium complexes.

2 Methods of calculation

The same methods as those described in our previous paper[57] were employed. The geometrical structures of the lowest triplet state (T_1) were optimized using the unrestricted DFT method, in which the B3LYP functionals[60] together with the SBKJC effective core potentials and associated basis sets[61,62] were used. In order to obtain more flexibility for theoretical description, the basis sets were augmented by a set of polarization functions[63] and referred to as SBKJC+p in this series of our investigations. The optimized structures were examined by normal-mode analyses and confirmed to be energy minima on their lowest triplet potential energy surfaces. Note that the expectation value of electron spin operator $\left\langle \hat{S}^2 \right\rangle$ has been found to be very close to two $\left(2.011 < \left\langle \hat{S}^2 \right\rangle < 2.041\right)$ except for the cases of introduction of NO_2 substituents $\left(\left\langle \hat{S}^2 \right\rangle = 2.065\right)$.

At these stationary geometries, the molecular orbitals were optimized using the MCSCF method[58] together with the state-averaging technique. The MCSCF active space includes six electrons and six orbitals, three of the orbitals mainly having an Ir *d* character and the remaining three orbitals having ligands' π character (principally anti-bonding) [MCSCF(6e,6)]. The electronic density was averaged among the lowest ten singlet and nine triplet states during MCSCF iterations. In order to describe electronically excited states and estimate the SOC effects among those states, SOCI wave functions[59] were constructed using the MCSCF optimized orbitals, in which the external space could include only 30 orbitals that have the lowest eigenvalues of the standard MCSCF Fock operator, due to our computer resource limitations. All calculations were achieved using the GAMESS suite of program codes[64].

Note that the words "HOMO" and "LUMO" are inappropriate since a set of natural orbitals optimized by the MCSCF method was used in the present investigation.[65] However, for simplicity, these words will be used as our current definitions in the following discussion: HOMO means the natural orbital for which the occupation number is *larger than one and the smallest* among them in the ground state, and LUMO means the natural orbital for which the occupation number is *smaller than one and the largest* among them in the ground state.[66] Additionally, it should be described that the energies of natural orbitals can be considered to be reversely proportional to their occupation numbers.

3 Results and discussion

Before starting discussion on the results of calculation for various iridium complexes, it should be noted that the dependency of lowest triplet geometries on the type of density functionals was examined. Typical functionals, B3LYP, M06[67] and PBE0,[68] were examined in the present investigation. The MCSCF+SOCI results of phosphorescent peak wavelengths suggest that B3LYP

geometries optimized for the lowest triplet states provide moderately good predictions in comparison with the M06 and PBE0 geometries, even though this functional is not corrected with respect to long-range interaction. Thereby, the following MCSCF-based calculations were performed for the B3LYP geometries optimized for the lowest triplet state in target complexes. Additionally, the present calculations were performed only for *fac* isomers of all $Ir(C^N)_3$, where C^N represents a ligand coordinating to iridium atom by carbon and nitrogen atoms such as a ppy ligand. This is because the *fac* isomer of the parent molecule $Ir(ppy)_3$ is more stable than the corresponding *mer* isomer (**Table 1**) and is known to have better phosphorescent efficiency than that for the corresponding *mer* isomer[69–77].

As described in our previous paper[76], in order to reproduce experimental emission spectra, it is necessary to consider spectral broadening and anharmonicity caused by the interaction with its circumstances and the geometrical displacement between the energy minima of electronic states. However, it is too time-consuming to calculate the potential energy curves (PECs) of low-lying spin-mixed (SM) states in many complexes and it becomes difficult to obtain the wavefunctions for energetically high vibrational states in each SM state. Therefore, we decided that the peak positions of emission spectra can be assumed to be provided by the superposition of Lorentz functions centered at the electronic transition energies from excited SM states to the ground state (SM0). In these calculations, the thermal population distribution for low-lying SM states was assumed to be given at an appropriate temperature and a Lorentz function for each electronic transition was assumed to have an appropriate half-value width.[77]

3.1 Brief Review on the effects of an F substituent and theoretical explanation

Introduction of F substituents to the Z_4 and Z_6 sites of phenyl rings (**Figure 1**) is known to be effective for a blue shift of the phosphorescent peaks in $Ir(ppy)_3$.[72–75] In our previous paper, the effects of F substituents were examined for the phosphorescence in several kinds of iridium complexes.[57] As reported in that paper,[57] $Ir(4\text{-}Fppy)_3$ (Z_4=F, Z_3=Z_5=Z_6=H) was calculated to have a phosphorescent peak at the wavelength of 456 nm, and $Ir(6\text{-}Fppy)_3$ (Z_6=F, Z_3=Z_4=Z_5=H) was also calculated to have a peak at the wavelength of 475 nm. As reported in our previous paper, the main contribution to the spectral peak in $Ir(4\text{-}Fppy)_3$ are the transition from SM4 to the ground state (455 nm) and that from SM3 to the ground state provides a small shoulder near the wavelength of 462 nm, where the principal components of SM3 and SM4 are S_1 and T_1, respectively, as shown in **Table2**, together with popular TD DFT results. It should be noted here that, even though the principal component of SM3 is S_1, the weight of T_1 is relatively large and the total weight of triplet states is larger than those of singlet states in SM3. Similarly, the main contribution in $Ir(6\text{-}Fppy)_3$ is the transition from SM4 to the ground state (474 nm) and the secondary contribution is that from SM3 to

the ground state (483 nm) (**Table 2** and **Figure 2**). On the other hand, Ir(5-Fppy)$_3$ (Z_5=F, Z_3=Z_4=Z_6=H) was calculated to have peaks at the wavelengths of 504 and 517 nm. Since Ir(3-Fppy)$_3$ (Z_3=F, Z_4=Z_5=Z_6=H) was predicted to have phosphorescent peaks at the wavelengths of 477 and 486 nm (the main contributions are the transitions from SM3 to the ground state (487 nm) and from SM4 to the ground state (477 nm)), the most effective position is proved to be the Z_4 site for a blue shift of the phosphorescence. It should be noted that similar results were obtained for the introduction of Cl (chlorine) substituents in the present investigation, although the magnitudes of the spectral shifts were smaller than those for the introduction of F substituents and those results are not included in the present paper.

The results[57] for the introduction of F substituents can be crudely explained as follows. The main component of the phosphorescence in such heavy-metal complexes is $d-\pi^*$ transition or metal-to-ligand charge-transfer (MLCT). As illustrated in **Figure 3**, the LUMO (see the last paragraph in Section 2 consists mainly of the lowest π^* orbital of the ligands[66] and has larger linear-combination-of-atomic-orbitals (LCAO) coefficients at the Z_4 and Z_6 sites of the phenyl rings of the ppy ligands, while negligible coefficients appear at the Z_3 and Z_5 sites. The blue shift of the phosphorescence is explained by energetically lifting the LUMO caused by introduction of F substituents to the Z_4 and Z_6 sites (**Figure 4(a)**). On the other hand, introduction to the Z_3 and Z_5 sites rarely affects the LUMO because of small coefficients (**Figure 3**). The steric effects might explain the blue shift in Ir(3-Fppy)$_3$, but it is apparent that Ir(5-Fppy)$_3$ has weak steric effects in the vicinity of the Z_5 sites. When the HOMO was examined carefully in the parent molecule Ir(ppy)$_3$, it was found to have non-zero coefficients at the Z_5 site (**Figure 3**). This orbital can interact with the occupied $2p\pi$ orbitals of F substituents, and this interaction lifts the HOMO energetically (**Figure 4(a)**). This is the reason why a red shift is predicted in Ir(5-Fppy)$_3$.

3.2 NH_2 substituent

In the present investigation, the similar tendency of spectral shifts was obtained when an electron-donating substituent NH_2 was introduced into phenyl rings of the ppy ligands (**Table 2** and **Figure 2**). In the present investigation, NH_2 substituent is a model of NX_2 groups, where X is assumed to be an appropriate bulky functional group but to rarely have the ability of π conjugation. When NH_2 substituents were introduced to the Z_4 or Z_6 site of the ppy ligands, the blue shifts of 49 and 9 nm was obtained respectively. On the other hand, a red shift (35 and 55 nm) was obtained for the introduction to the Z_5 site, where two spectral peaks appear at the wavelengths of 526 and 546 nm and those correspond to the transitions from SM4 and SM3 to the ground state, respectively (**Table 2**). These magnitudes of spectral shifts are apparently larger than those for the introduction of F substituents. These results can be explained as follows: the sum of two C–N–H angles and one

H–N–H angle for each NH_2 substituent at the DFT structures optimized for the lowest triplet states is apparently larger than the corresponding sum for an NH_3 molecule ($107.3 \times 3 = 322$ degree): especially, one of NH_2 substituents in Ir(3-NH_2ppy)$_3$ has an angle close to 360 degree (planar) and is located on the π plane provided by the adjacent ppy ligand (**Table 3** and **Figure 5**). Accordingly, effective π interaction must occur between π orbitals of the ppy ligands and the lone-pair orbital at the NH_2 substituents. Under such circumstances, since the lone-pair orbital can play a role of occupied π orbital in these complexes and is higher in energy than the F's $2p\pi$ occupied orbital, the energetic shift of HOMO shown in **Figure 3**(a) must be larger than that in the isomers of Ir(Fppy)$_3$. Thus, the same tendency was obtained for the introduction of electron-withdrawing F and electron-donating NH_2 substituents and it can be understood that large magnitudes of the spectral shifts were obtained by such strong π interactions in the isomers of Ir(NH_2ppy)$_3$.

Experimental reports have been published on the effects of introducing diphenyl-amino (NPh_2) groups to the Z_4 sites.[78–80] The introduction of NPh_2 groups corresponds to forming parts of starburst materials for OLEDs. If a bridged bond between two phenyl rings, it becomes a popular carbazole substituent. The peak of emission spectra in Ir(4-NPh_2-ppy)$_3$ is reported to be observed at the wavelength of 526–534 nm,[78–80] so that the magnitude of red-shift is about 20 nm. This could be interpreted as the strong $\pi - \pi$ interaction between the terminal phenyl groups of NPh_2 and ppy ligands. As described above, we assumed to exclude such situation of strong π conjugation. Thus, it should be understood that the effects of phenyl groups are so important as those of nitrogen atoms of NPh_2. Unfortunately, NPh_2 groups are too large for us to carry out theoretical calculations at the present levels of theory because of our computer resources.

3.3 NO_2 and CN substituents

NO_2 and CN substituents are known to be strong electron-withdrawing substituents. The present investigation selected these substituents for the purpose of examining the magnitudes of spectral shifts of the phosphorescence. Although the most stable isomer is Ir(4-Zppy)$_3$ when Z = F or NH_2, Ir(5-Zppy)$_3$ is more stable than the other isomers, Ir(3-Zppy)$_3$, Ir(4-Zppy)$_3$ and Ir(6-Zppy)$_3$ in the cases of Z = NO_2 and CN. The relative stabilities of these isomers can be explained by the energetic shifts of HOMO shown in **Figure 4**. As described the details in the following discussion, the energy of HOMO is almost unchanged in Ir(4-Zppy)$_3$ and Ir(6-Zppy)$_3$ in the case of Z = F or NH_2, but it is lifted in Ir(5-Zppy)$_3$.[66] On the other hand, the HOMO is also unchanged approximately in Ir(4-Zppy)$_3$ and Ir(6-Zppy)$_3$ in the case of Z = NO_2 or CN, while it is lowered in Ir(5-Zppy)$_3$ (Z = NO_2 or CN).

Likewise, the effects of NO_2 and CN substituents to spectral peak shifts are completely different from those of F and NH_2 substituent as shown in **Table 2** (and **Figure 2**). When one of

these substituents is introduced to each Z_4 site (Ir(4-Zppy)$_3$), the phosphorescent peaks are split into two and shifted to the red region by 96 and 70 nm (Z=NO_2) or 48 and 31 nm (Z=CN) nm. These peaks are assigned to the transitions from SM3 and SM4 to the ground state. In the same manner, when it is introduced to the Z_6 site (Ir(6-Zppy)$_3$), the phosphorescent peak is calculated to be considerably shifted to the red region. These peaks are also split into two, respectively; the magnitudes of red shift are 159 and 153 nm for Z=NO_2, and 43 and 30 nm for Z=CN. These peaks are also assigned to the transitions from SM3 and SM4 to the ground state, respectively, where the principal components of SM3 and SM4 are S_1 and T_1, respectively (see **Table2**) and, even though the principal component of SM3 is S_1, the weight of T_1 is relatively large and the total weight of triplet states is larger than those of singlet states in SM3. The key difference among these substituents is the existence of low-lying π^* orbitals. Only the *3p* orbital can play a role of a π^* orbital in F substituent and is apparently high in energy. An orbital in NH_2 substituent, which is expected to play a role of π^* orbital at a structure close to a planar one, must be high in energy than the π^* orbitals of electron-withdrawing NO_2 and CN substituents. As mentioned above, the LUMO in the parent molecule Ir(ppy)$_3$ has large coefficients at the Z_4 and Z_6 sites and can strongly interact with the π^* orbitals of these substituents (**Figure 3**). Additionally, when the NO_2 substituent is introduced to the Z_4 site, attractive interaction[81] can occur between the oxygen atoms of the NO_2 substituent and the adjacent hydrogen atoms of the phenyl rings. These bonds must enhance the π conjugation between the ligands and the substituents and make the magnitude of the red shift larger (**Figure 4(b)**). In fact, all three atoms of the NO_2 substituent are located on the π plane provided by the ppy ligands in Ir(4-NO_2ppy)$_3$ (**Figure 6**). This geometrical feature must be the reason why such large red shifts are obtained in these complexes. The magnitude of the red shift in Ir(4-CNppy)$_3$ is smaller than that in Ir(4-NO_2ppy)$_3$, since attractive interaction is negligible between the terminal nitrogen atoms of CN substituent and the adjacent hydrogen atoms of the phenyl rings in Ir(4-CNppy)$_3$.

With respect to π interaction between ligands and substituents and to attractive interaction between hydrogen atoms and adjacent oxygen or nitrogen atoms, the situation in Ir(6-Zppy)$_3$ is similar to that in Ir(4-Zppy)$_3$ (Z = NO_2 or CN). Additionally, the Z_6 sites are geometrically close to the adjacent pyridine rings or geometrically crowded, so that the NO_2 substituents are somewhat displaced from the π planes of the ligands in order to minimize nuclear repulsion (**Figure 6**). Nevertheless, attractive interaction[81] still exists between the oxygen atoms of the NO_2 substituent and the adjacent hydrogen atoms of the ligands, and π conjugation occurs in the larger space including pyridine rings. The large red shift (153/159 nm) in Ir(6-NO_2ppy)$_3$ must be attributed to this large space of π conjugation including both phenyl and pyridine rings. Thus, the introduction

of these substituents to the Z_4 and Z_6 sites makes the LUMO explicitly lower in energy than that in the parent molecule $Ir(ppy)_3$ (**Figure 4(b)**)[66] and, as a result, it causes a relatively large red shift of the phosphorescent peaks in $Ir(6\text{-}Zppy)_3$ as well as $Ir(4\text{-}Zppy)_3$ (Z = NO_2 or CN).

On the other hand, when one of these electron-withdrawing substituents is introduced to the Z_5 site [$Ir(5\text{-}Zppy)_3$], the phosphorescent peak is split into two and shifted to the blue region by 87 and 95 nm for Z = NO_2, while it is shifted to the blue region by 32 nm for Z = CN (**Table 2**). As mentioned above, the Z_5 site in the parent molecule $Ir(ppy)_3$ has negligible coefficients in LUMO but has non-negligible coefficients in HOMO (**Figure 3**), so that introduction of the substituents to the Z_5 sites causes a meaningful interaction between the HOMO of the parent molecule $Ir(ppy)_3$ and the π^* orbitals of the substituents (**Figure 4(b)**).[82] Since the main components of the HOMO in these complexes are Ir's d orbitals, the coefficients at the Z_5 sites of the ppy ligands in HOMO are explicitly smaller than those at the Z_4 and Z_6 sites in LUMO of the parent molecule $Ir(ppy)_3$. This might be the reason why the magnitudes of the blue shifts are smaller than those of the red shift in $Ir(4\text{-}Zppy)_3$ and $Ir(6\text{-}Zppy)_3$. This interaction is also enhanced by the attractive interaction between the oxygen atoms of NO_2 substituents and the adjacent hydrogen atoms of the ligands,[81] since such an attractive interaction makes the NO_2 substituents located on the π plane of the ligands (**Figure 6(c)**). Thus, it can be understood that, in addition to the electron-withdrawing effects of these substituents, the interaction between the HOMO of the parent molecule $Ir(ppy)_3$ and the π^* orbitals of the substituents makes HOMO lower in energy[66] in the target molecule (**Figure 4(b)**[82]) and, as a result, a blue shift of the phosphorescence was obtained by the introduction of these substituents to the Z_5 sites. Since the π^* orbitals in the NO_2 substituent lower HOMO in energy than that in the CN substituent,[66] the magnitude of the blue shift in $Ir(5\text{-}NO_2ppy)_3$ is calculated to be large in comparison with that in the $Ir(5\text{-}CNppy)_3$.

In order to examine the rates of non-radiative transitions in these complexes, geometrical displacements between the ground state and the lowest triplet state[83] were also calculated. In most of the present complexes, the geometrical displacements were calculated to be 0.04 – 0.08 Å/atom. Since these displacements are comparable with that in the *fac* isomer of the parent molecule $Ir(ppy)_3$ and is apparently smaller than that in the *mer* isomer, fast non-radiative transition is not expected to occur in these complexes. When NO_2 substituents were introduced to the Z_3 sites, an unexpected bond was formed between the terminal oxygen atoms of NO_2 substituents and the closest carbon atoms of the adjacent ligand during geometry optimization for the lowest triplet state (indicated by a dotted circle in **Figure 6(a)**). As a result, the ring of the ligand becomes pyramidal (non-planar sp^3 structure). This is the reason why $Ir(3\text{-}NO_2ppy)_3$ was excluded from the present investigation.[84] Such behavior of NO_2 substituent may be the reason why it has not been used in experiments so far.

Unfortunately, no experimental reports could be found for Ir(5-Zppy)$_3$ (Z = NO_2 or CN). As described in the next section, experimental observation suggests that introduction of CN substituents to the Z_5 sites in tris(4,6-difluoro- 2-phenylpyridinato)iridium(III) [*fac*-Ir(4,6-dfppy)$_3$] causes a blue shift of 27 nm (from 469 to 442).[85] This is in good agreement with the present results of calculation for Ir(5-CNppy)$_3$ with respect to the magnitude of spectral shift (from 491 to 459). It is therefore said that Ir(5-NO_2ppy)$_3$ must be the best doping material for blue color emission. When the observation at room temperature[72] is taken as a reference (see **Table 2**), the present computational method underestimates the peak wavelength by 24 nm in the parent molecule Ir(ppy)$_3$. If this difference is applicable to the other computational results, the phosphorescent peaks in Ir(5-NO_2ppy)$_3$ are predicted to be observed near the wavelengths of 420 and 428 nm. Thus, we would conclude that Ir(5-NO_2ppy)$_3$ is the best phosphorescent complex, but, if NO_2 substituent is troublesome to use for a dopant, the secondary selection must be Ir(5-CNppy)$_3$. However, the predicted wavelength is 483 nm after correction of the present computational underestimation. These wavelengths are too long to employ it as a blue-color emissive material. Therefore, better combinations of substituents will be examined in the next section. At the end of this section, we should emphasize that the most important point of the substituent effects is not electron-withdrawing strength but the existence of low-lying π^* orbitals in substituents, though this comment may be same meaning when substituents have a π plane.

3.4 Combination effects of substituents

Based on the results and discussion in the previous section, better combinations of substituents for blue phosphorescence will be examined in this section. We have two groups of substituents: (i) Z = F or NH_2 and (ii) Z = NO_2 or CN. For the purpose of obtaining blue-color emission, Group (i) should be introduced to the Z_4 and/or Z_6 sites, while Group (ii) should be done to the Z_5 site. Then, we take tris(4,6-difluoro-2-phenylpyridinato)iridium(III) [Ir(4,6-dfppy)$_3$] and tris(4,6-diamino-2-phenylpyridinato)iridium(III) [Ir(4,6-dappy)$_3$] as parent molecules in the present section and discuss spectral shifts when NO_2 or CN is introduced to the Z_5 site. As mentioned in the previous section, only the *fac* isomers of all complexes are considered in the following sections.

3.4.1 Substituent effects in Ir(4,6-dfppy)$_3$

As already reported in our previous paper, the spectral peaks are calculated to appear at the wavelengths of 440 and 446 nm in Ir(4,6-dfppy)$_3$ (see **Figure 7**(a)).[57] When a thermal distribution is considered among the low-lying excited spin-mixed states, the main peak appears at the wavelength of 440 nm and, in other words, it is shifted to the blue region by 51 nm when all three ppy ligands are replaced by 4,6-dfppy ligands. Experimental observation[71,73-77] indicates that the

spectral peak appears at the wavelength of 468 – 469 nm, so that the magnitude of the blue shift is 46–47 nm. Accordingly, the magnitude of the blue shift caused by the replacement of three ppy ligands by 4,6-dfppy ligands is overestimated only by 4–5 nm in the present calculations. In consideration of underestimating the peak wavelength for $Ir(ppy)_3$ by 24 nm described at the end of the previous section, we assume that the present method underestimates peak wavelengths by 24–29 nm for iridium complexes in the following discussion.

Table 2 shows the results of calculation for Ir(5-Z-4,6-dfppy)$_3$ (Z_5 = NO_2 or CN). The magnitudes of the blue shift caused by introduction of the substituents are calculated to be 66 nm for Z_5 = NO_2 and 31 nm for Z_5 = CN, where these peaks are obtained as the overlaps of the transitions from two or three SM states to the ground state, where all these SM states has largest weights of triplet states, even though the principal component is S_1 in SM3 (see **Table 2**). As already mentioned in the previous section, the magnitude of the blue shift is in good agreement with the experimental observation[85] for Ir(5-CN-4,6-dfppy)$_3$ after considering the present computational underestimation. Only when NO_2 substituents are introduced to the Z_5 site, is the magnitude reduced by 29 nm, even though the magnitude of the blue shift itself is still largest. This result can be easily understood: since no attractive interaction can occur between this substituent and the adjacent F substituents, in contrast to the case of $Ir(ppy)_3$, NO_2 substituents rotate around the C-N bonds and their oxygen atoms are displaced from the π plane provided by each ppy ligand (**Figure 8**). Such geometrical rotation weakens the π interaction between the substituents and the 4,6-dfppy ligands. This must be the reason why the magnitude of the blue shift is reduced by 29 nm in Ir(5-NO_2-4,6-dfppy)$_3$. Nevertheless, the introduction of these substituents can cause effective blue shifts, and the spectral peak in Ir(5-NO_2-4,6-dfppy)$_3$ appears in the region of shorter wavelength (374 nm). This wavelength may be too short for blue-color emission, where correction of the present computational underestimation suggests that the spectral peak appears at the wavelengths of 398–403 nm. If NO_2 substituent could be troublesome to use for a dopant, a better candidate would be Ir(5-CN-4,6-dfppy)$_3$ rather than Ir(5-NO_2-4,6-dfppy)$_3$. This conclusion is consistent with the fact that the experimental observation (442 nm)[85] has been reported for Ir(5-CN-4,6-dfppy)$_3$.

Before finishing this subsection, it would be noteworthy to describe the effects of the third F substituent. When the third F substituent is introduced to the Z_3 site in Ir(6-NO_2-4,6-dfppy)$_3$, strong π conjugation occurs between NO_2 substituent and the adjacent pyridine ring and makes the spectral peak shift to red region in Ir(6-NO_2-4,6-dfppy)$_3$ unfortunately. On the other hand, when the third F substituent[86] is introduced to the Z_3 sites in Ir(5-CN-4,6-dfppy)$_3$, the spectral peak is calculated to appear at the wavelength of 406 nm (**Figure 7**(b)). Namely, the third F substituent provides a small magnitude of blue shift (3 nm) and helps to obtain brighter blue-color emission. After correction of the present computational underestimation, the spectral peak is estimated to

appear at the wavelength of 430–435 nm for Ir(5-CN-3,4,6-tfppy)$_3$. Note that since the geometrical displacements caused by electronic transitions are calculated to be 0.03 – 0.06 Å/atom for these complexes, fast non-radiative transition can be considered to rarely occur in these complexes.

3.4.2 Substituent effects in Ir(4,6-dappy)$_3$

Based on the discussion in Sections 3.1–3.3, NH_2 substituent is the more effective than F substituent for a blue shift of spectral (phosphorescent) peaks, when it is introduced to the Z_4 site. Additionally, a small blue shift was also obtained when NH_2 substituent is introduced to the Z_6 site. Therefore, we discuss the combination effects of NH_2 substituents with NO_2 or CN substituent in this section.

When two NH_2 substituents are introduced to the Z_4 and Z_6 sites (Ir(4,6-dappy)$_3$), the spectral peaks are calculated to appear at the wavelength of 440 nm (**Table 2** and **Figure 7(c)**). As mentioned in Section 3.2, since Ir(4-NH_2ppy)$_3$ has a peak at the wavelength of 442 nm and the introduction of NH_2 substituent to the Z_6 site causes a small blue shift (9 nm), it is understandable that the peak in Ir(4,6-dappy)$_3$ appears at the wavelength of 440 nm.

As mentioned above, when an NH_2 substituent is introduced to the Z_4 and Z_6 sites, the LUMO is lifted by the interaction between the lone-pair orbitals of NH_2 substituents and the LUMO of the parent molecule Ir(ppy)$_3$. At the same time, the lone-pair orbitals of NH_2 substituents interact with ligands' π orbitals, and such interaction between occupied π orbitals makes ligands' π orbitals higher in energy and closer in energy to the HOMO (principally occupied Ir's d orbitals). Under such circumstances, the introduction of an NO_2 or CN substituent to the Z_5 site makes the HOMO lower in energy as shown in **Figure 4(b)**.[82] As a result, though we finally succeed in obtaining a large blue shift for Ir(5-CN-4,6-dappy)$_3$ as shown in **Table 2**, the HOMO (Ir's d orbitals) were largely lowered by these interactions and it becomes closer in energy to occupied π orbitals of the ligands. As a result, their energetic order has been changed during MCSCF iterations in Ir(5-NO_2-4,6-dappy)$_3$. We recalculated several times in order to maintain Ir's d-orbital character in MCSCF active space for Ir(5-NO_2-4,6-dappy)$_3$, but the MCSCF active orbitals always lose Ir's d-orbital components and become pure π orbitals of the ligands in Ir(5-NO_2-4,6-dappy)$_3$. This fact suggests that some $(\pi - \pi^*)$ excited states are explicitly lower in energy than MLCT $(d - \pi^*)$ excited states in this complex and that SOC mixing between low-lying singlet and triplet states rarely occurs and only very weak or almost no phosphorescence can be observed in Ir(5-NO_2-4,6-dappy)$_3$ (see **Figure 7**(c)). Thus, we unfortunately have to conclude that Ir(5-NO_2-4,6-dappy)$_3$ is inappropriate but Ir(5-CN-4,6-dappy)$_3$ could be used as phosphorescent materials.

4 Summary

The substituent effects on emission in *fac*-Ir(ppy)$_3$ and its derivatives were examined theoretically by using the MCSCF+SOCI/SBKJC+p method followed by SOC calculations. The strongest electron-donating substituent NH_2 and the strongest electron-withdrawing substituents, NO_2 and CN, were chosen for investigating the substituent effects. It was found that when NO_2 or CN substituent is introduced to the Z_5 sites, the largest blue shift is obtained for the emission spectra, while F and NH_2 substituent provide a red shift. This is because the Z_5 site has negligible coefficients in LUMO but has small coefficients in HOMO in *fac*-Ir(ppy)$_3$. Although F and NH_2 substituent do not have low-lying π^* orbitals, NO_2 and CN substituents have low-lying π^* orbitals and, therefore, the HOMO is energetically lowered by the introduction of these substituents to the Z_5 sites (**Figure 4(b)**)[82] and a large blue shift of the emission peak is expected to be obtained, especially when NO_2 substituent is introduced. Therefore, it can be said that the best material for blue-color emission is *fac*-Ir(5-NO_2ppy)$_3$ or *fac*-Ir(5-NO_2-4,6-dfppy)$_3$. Since geometry optimization for the lowest triplet state in *fac*-Ir(3-NO_2ppy)$_3$ provided an unexpected bond between a terminal oxygen atom of one of NO_2 substituents and its adjacent ppy ligand, the introduction of NO_2 substituents could be troublesome in synthetic processes and/or in emissive layers of OLEDs. If this is the reason why NO_2 substituents have never been used for OLED, we suggest that *fac*-Ir(5-CN-3,4,6-tfppy)$_3$ is the most appropriate for blue-color emission. The present investigation focused on the electronic transitions in molecules doped into emissive layers, but it is necessary to consider interactions between the molecules and host molecules in emissive layers of OLEDs. Such interactions are the targets in another series of our investigations.[87–92] On the basis of these successes, the substituent effects in bis[2-(phenyl)pyridinato-N,C2'] [picolinato-N,O] iridium(III) [Ir(ppy)$_2$(pic)] and bis[2-(phenyl)pyridinato-N,C2'] [2,4-pentanedionato-O,O] iridium(III) [Ir(ppy)$_2$(acac)] are under investigation in our laboratory in order to find better complexes for solution-processed OLEDs.

References

1 C. W. Tang, S. W. Van Slyke, C. H. Chen, *J. Appl. Phys.* 1989, **65**, 3610–3616.

2 K. Pier: Pierloot, A. Ceulemans, M. Merchán, L. Serrano-Andrés, *J. Phys. Chem. A* 2000, **104**, 4374–4382.

3 J. Brooks, Y. Babayan, S. Lamansky, P. I. Djurovich, I. Tsybam, R. Bau, M. E. Thompson, *Inorg. Chem.* 2002, **41**, 3055–3066.

4 X. Gu, T. Fei, H. Zhang, H. Xu, B. Yang, Y. Ma, X. Liu, *J. Phys. Chem.* 2008, **112**, 8387–8393.

5 X. Li, Z. Wu, X. Li, H. Zhang, X. Liu, *J. Comput. Chem*., 2011, **32**, 1033–1042.

6 J. Wang, B. Xia, F. Bai, L. Sun, H. Zhang, *Int. J. Quantum Chem.* 2011, **111**, 4080–4090.

7 A. Kadari, A. Moncomble, I. Ciofini, M. Brahimi, C. Adamo, *J. Phys. Chem*. A 2011, **115**, 11861–11865.

8 E. Baranoff, B. F. E. Curchod, J. Frey, R. Scopelliti, F. Kessler, I. Tavernelli, U. Rothlisberger, M. Grätzel, M. K. Nazeeruddin, *Inorg. Chem.* 2012, **51**, 215–224.

9 Y. Su, L. Kang, *Int. J. Quantum Chem.* 2012, **112**, 2422–2428.

10 J. Su, X. Sun, G. Gahungu, X. Qu, Y. Liu, Z. Wu, *Syn. Metals*, 2012, **162**, 1392–1399.

11 Q. Cao, J. Wang, Z. Tian, Z. Wie, F. Bai, *J. Comp. Chem.* 2012, **33**, 1038–1046.

12 H. Li, P. Winget, C. Risko, J. S. Sears. J. Bredas, *Phys. Chem. Chem. Phys*., 2013, **15**, 6293–6302.

13 D. Han, G. Zhang, H. Cai, X. Zhang, L. Zhao, *J. Luminescence*, 2013, **138**, 223–228.

14 X. Shang, D. Han, D. Li, Z. Wu, *Chem. Phys. Lett.* 2013, **565**, 12–17.

15 X. Shang, Y. Liu, X. Qui, Z. Wu, *J. Luminescence*, 2013, **143**, 402–408.

16 X. Shang, D. Han, D. Li, S. Guan, Z. Wu, *Chem. Phys. Lett*., 2013, **588**, 68–75.

17 X. Shang, Y. Liu, J. Su, G. Gahungu, X. Qu, Z. Wu, *Int. J. Quantum Chem*. 2014, **114**, 183–191.

18 Y. Si, X. Sun, Y. Liu, X. Qu, Y. Wang, Z. Wu, *Dalton Trans.* 2014, **43**, 714–721.

19 Y. Si, Y. Liu, X. Qu, Y. Wang, Z. Wu, *Dalton Trans*., 2013, **42**, 14149–14157.

20 J. Younker, J. M.; Dobbs, K. D. Correlating Experimental Photophysical Properties of Iridium(III) Complexes to Spin-Orbit Coupled TDDFT Predictions. *J. Phys. Chem. C* **2013**, *117*, 25714–25723.

21 R. Srivastava, Y. Kada, B. Kotamarthi, *Comput. Theoret. Chem.* 2013, **1009**, 35–42.

22 X. Qu, Y. Liu, G. Godefroid, Y. Si, X. Shang, X. Wu, Z. Wu, *Eur. J. Inorg. Chem*. **2013**, 3370–3383.

23 X. Qu, Y. Liu, Y. Si, X. Wu, Z. Wu, *Dalton Trans*., 2014, **43**, 1246–1260.

24 M. Song, Z. Hao, Z. Wu, S. Song, I. Zhou, R. Deng, H. Zhang, *J. Phys. Org. Chem*. 2013, **26**, 840–848.

25 Y. Li, L. Zou, A. Ren, M. Ma, J. Fan, *Chem. Eur. J*., 2014, **20**, 4671–4680.

26 D. Han, C. Li, L. Zhao, X. Sun, G. Zhang, *Chem. Phys. Let.* 2014, **595–596**, 260–265.

27 K. Mori, T. P. M. Goumans, E. Lenthe, E. Wang, *Phys. Chem. Chem. Phys*. 2014, 16, 14523–14530.

28 L. Wang, Y. Wu, G. Shan, Y. Geng, J. Zhang, D. Wang, G. Yang, Z. Su, *J. Mater. Chem. C*, 2014, **2**, 2859–2868.

29 B. F. Minaev, S. Knuts, H. Agren, O. Vahtras, *Chem. Phys.* 1993, **175**, 245–254.

30 H. Agren, O. Vahtras, B. F. Minaev, *Adv. Quantum Chem.* 1996, **27**, 71–162.

31 B. F. Minaev, *Opt. Spectrosc.* 2005, **98**(3), 336–340.

32 B. F. Minaev, E. Jansson, H. Ågrena, S. Schrader, *J. Chem. Phys.* 2006, **125**, 234704-1–18.

33 E. Jansson, B. Minaev, S. Schrader, H. Ågren, *Chem. Phys.* 2007, **333**, 157−167.

34 B. Minaev, V. Minaeva, H. Ågren, *J. Phys. Chem. A* 2009, **113**, 726–735.

35 B. Minaev, H. Ågren, F. de Angelis, *Chem. Phys.* 2009, **358**, 245−257.

36 X. Li, B. Minaev, H. Ågren, H. Tian, *J. Phys. Chem.* C 2011, **115**, 20724−20731.

37 X. Li, B. Minaev, H. Ågren, H. Tian, *Eur. J. Inorg. Chem.* 2011, 2517−2524.

38 D. Volyniuk, V. Cherpak, P. Stakhira, B. F. Minaev, G. V. Baryshnikov, M. Chapran, A. Tomkeviciene, J. Keruckas, J. V. Grazulevicius, *J. Phys. Chem.* C, 2013, **117**, 22538–22544.

39 B. F. Minaev, G. Baryshnikov, H. Agren, *Phys. Chem. Chem. Phys.* 2013, **16**, 1719–1758.

40 V. Cherpak, P. Stakhira, B. Minaev, G. Baryshnikov, E. Stromylo, I. Helzhynskyy, M. Chapran, D. Volyniuk, D. Tomkuté-Lukšiené, T. Malinauskas, V. Getautis, A. Tomkeviciene, J. Simokaitiene, J. V. Grazulevicius, *J. Phys. Chem. C* 2014, **118**, 11271–11278.

41 S. Koseki, M. W. Schmidt, M. S. Gordon, *J. Phys. Chem.* 1992, **96**, 10768–10772.

42 S. Koseki, M. S. Gordon, M. W. Schmidt, N. Matsunaga, *J. Phys. Chem.* 1995, **99**, 12764–12772.

43 N. Matsunaga, S. Koseki, M. S. Gordon, *J. Chem. Phys.* 1996, **104**, 7988–7996.

44 S. Koseki, M. W. Schmidt, M. S. Gordon, *J. Phys. Chem.* A 1998, **102**, 10430–10435.

45 S. Koseki, D. G. Fedorov, M. W. Schmidt, M. S. Gordon, *J. Phys. Chem.* A 2001, **105**, 8262–8268.

46 D. G. Fedorov, S. Koseki, M. W. Schmidt, M. S. Gordon, *Int. Rev. Phys. Chem.* 2003, **22**, 551–592.

47 D. G. Fedorov, M. W. Schmidt, S. Koseki, M. S. Gordon, *Recent Advances in Relativistic Molecular Theory*, World Scientific, Singapore, **2004**, Vol. 5, pp. 107–136.

48 S. Koseki, Y. Ishihara, U. Umeda, D. G. Fedorov, M. S. Gordon, *J. Phys. Chem.* A 2002, **106**, 785–794.

49 S. Koseki, Y. Ishihara, H. Umeda, D. G. Fedorov, M. W. Schmidt, M. S. Gordon, *J. Phys. Chem.* A 2004, **108**, 4707–4719.

50 S. Koseki, T. Matsushita, M. S. Gordon, *J. Phys. Chem.* A 2006, **110**, 2560–2570.

51 S. Koseki, *Computational Methods in Sciences and Engineering, Theory and Computation: Old Problems and New Challenges*, edited by George Maroulis and Theodore Simos, AIP, New York, **2008**, CP963, Vol. 1, page 257–267.

52 S. Koseki, N. Shimakura, Y. Fujimura, T. Asada, H. Kono, *J. Chem. Phys.* 2009, **131**, 044122-1–8.

53 T. Hisashima, T. Matsushita, T. Asada, S. Koseki, *Theoret. Chem. Acc.* 2008, **120**, 85–94.

54 S. Koseki, T. Hisashima, T. Asada, A. Toyota, N. Matsunaga, *J. Chem. Phys.* 2010, **133**, 174112-1–9.

55 T. Matsushita, T. Asada, S. Koseki, *J. Phys. Chem. A* 2006, **110**, 13295–13302.

56 T. Matsushita, T. Asada, S. Koseki, *J. Phys. Chem. C* 2007, **111**, 6897–6903.

57 S. Koseki, N. Kamata, T. Asada, S. Yagi, H. Nakazumi, T. Matsushita, *J. Phys. Chem. C* 2013, **117**, 5314–5327.

58 M. W. Schmidt, M. S. Gordon, *Annu. Rev. Phys. Chem.* 1998, **49**, 233−266.

59 B. H. Lengsfield III, J. A. Jafri, D. H. Phillips, C. W. Bauschlicher Jr., *J. Chem. Phys.* 1981, **74**, 6849–6856.

60 A. D. Becke, *J. Chem. Phys.* 1993, **98**, 5648–5652.

61 W. J. Stevens, H. Basch, M. Krauss, P. Jasien, *Can. J. Chem.* 1992, **70**, 612–630.

62 T. R. Cundari, W. J. Stevens, *J. Chem. Phys.* 1993, **98**, 5555–5565.

63 Exponents of 0.938 are used for *f* functions on Ir. The d exponents are 0.650 (S) and 0.800 (C and N). The p exponents are 1.100 (H). This basis set is referred to as SBKJC+p.

64 M. W. Schmidt, K. K. Baldridge, J. A. Boatz, S. T. Elbert, M. S. Gordon, J. H. Jensen, S. Koseki, N. Matsunaga, K. A. Nguyen, S. Su, T. L. Windus, M. Dupuis, J. A. Montgomery, *J. Comput. Chem.* 1993, **14**, 1347–1363.

65 "HONO" (highest occupied natural orbital) and "LUNO" (lowest unoccupied natural orbital) are sometimes used (for example, J. Hachmann, J. J. Dorando, M. Avilés, G. Kin-Lic Chan, *J. Chem. Phys.* 2007, **127**, 134309). However, we used HOMO and LUMO for simplicity.

66 Exactly speaking, the occupation number of HOMO is almost unchanged in Ir(4-Zppy)$_3$ and Ir(6-Zppy)$_3$ in the case of Z = F or NH_2, while the occupation number of HOMO decreases in Ir(5-Zppy)$_3$. The fact that the occupation number increases (decreases) indicates that the orbital energy is lowered (lifted) in MCSCF calculations.

67 Y. Zhao, D. G. Truhlar, *Theoret. Chem. Acc.* 2008, **120**, 215–241.

68 J. P. Perdew, K. Burke, M. Ernzerhof, *Phys. Rev. Lett.* 1996, **77**, 3865–3868. Err. **1997**, *78*,1396.

69 M. A. Baldo, S. Lamansky, P. E. Burrows, M. E. Thompson, S. R. Forrest, *Appl. Phys. Lett.* 1999, **75**, 4−6.

70 C. Adachi, M. A. Baldo, S. R. Forrest, *Appl. Phys. Lett.* 2000, **77**, 904−906.

71 A. B. Tamayo, B. D. Alleyne, P. I. Djurovich, S. Lamansky, I. Tsyba, N. N. Ho, R. Bau, M. E. Thompson, *J. Am. Chem. Soc.* 2003, **125**, 7377−7387.

72 H. Wang, Q. Liao, H. Fu, Y. Zeng, Z. Jiang, J. Ma, J. Yao, *J. Mater. Chem*. 2009, **19**, 89–96.

73 A. Beeby, S. Bettington, I. D. Samuel, Z. Wang, *J. Mater. Chem.* 2003, **13**, 80-83.

74 J. Frey, B. F. E. Curchod, R. Scopelliti, I. Tavernelli, U. Rothlisberger, M. K. Nazeeruddin, E. Baranoff, *Dalton Trans.* 2014, 43, 5667–5679.

75 K. Dedeian, J. Shi, N. Shepherd, E. Forsythe, D. C. Morton, *Inorg. Chem.* 2005, **44**, 4445–4447.

76 S. Koseki, Y. Kagita, S. Matsumoto, T. Asada, S. Yagi, H. Nakazumi, T. Matsushita, *J. Phys. Chem. C* 2014, **118**, 15412–15421.

77 The temperature and the spectral half-value width were assumed to be 400 K and 6 cm^{-1} for the purpose of reproducing the observed spectral shapes for fac-$Ir(ppy)_3$ and FIrpic, where all transitions from the excited states to the ground state were included when their emission energy smaller than 30,000 cm^{-1}. The temperature is set to be relatively high, since the MCSCF+SOCI calculations tend to overestimate emission energies because of relatively small active space.

78 K. Ono, M. Joho, K. Saito, M. Tomura, Y. Matsushita, S. Naka, H. Okada, H. Onnagawa, *Eur. J. Inorg. Chem.* 2006, 3676–3683.

79 G. Zhou, Q. Wang, C.-L. Ho, W.-Y. Wong, D. Ma, L. Wang, Z. Lin, *Chem. Asian J.* 2008, **3**, 1830–1841.

80 Y. Li, L.-Y. Zou, A.-M. Ren, M.-S. Ma, J.-X. Fan, *Chem. Eur. J.* 2014, **20**, 4671–4680.

81 At the DFT(B3LYP)/SBKJC+p level of calculation, the bond distances and bond orders between these two atoms are calculated to be 2.382–2.419 Å and 0.037–0.056 in $Ir(4\text{-}NO_2ppy)_3$, 2.341–2.446 Å and 0.033–0.041 in $Ir(5\text{-}NO_2ppy)_3$, and 2.214–2.597 Å and 0.001–0.039 in $Ir(6\text{-}NO_2ppy)_3$.

82 The π orbitals of the substituent Z (=NO_2 or CN) can also interact with the HOMO of the parent molecule $Ir(ppy)_3$ shown in **Figure 3**, when Z is introduced to the Z_5 site. However, in these π orbitals, the LCAO coefficients for N of NO_2 or those for C of CN are smaller than those for the terminal Os of NO_2 or the terminal N of CN. The magnitudes of LCAO coefficients are completely opposite in the π^* orbitals of the substituent Z. Therefore, the interaction between the Z's π^* orbital and the HOMO of the parent molecule must be more effective than those

between the Z's π orbital and the HOMO of the parent molecule, if their energy differences are not included into the present consideration.

83 After the mass centers of the geometries optimized for the ground state and the lowest triplet state are moved to the coordinate origin and the orientation of the complexes is aligned under the condition that rotational angular momentum should not be generated by geometrical displacement between the optimized geometries of the two states, the geometrical displacement is defined as $|\Delta Q| = \frac{1}{N}\sum_{i=1}^{N}\sqrt{\sum_{\alpha}^{x,y,z}\left(q_{i,\alpha}^{S0} - q_{i,\alpha}^{T1}\right)^2}$ (N being the number of atoms). Note that the equation in our previous paper [ref.57] is wrong.

84 We also succeeded in obtaining a reasonable structure for Ir(3-NO_2ppy)$_3$ without forming extra-bonds, but this structure was higher in energy than the structure shown in **Figure 6(a)**.

85 S. H. Kim, J. Jang, S. J. Lee, J. Y. Lee, *Thin Solid Films* 2008, **517**, 722–726.

86 R. Ragni, E. A. Plummer, K. Brunner, J. W. Hofstraat, F. Babudri, G. M. Farinola, F. Naso, L. de Cola, *J. Mater. Chem.* 2006, **16**, 1161–1170.

87 T. Asada, T. Takahashi, S. Koseki, *Theor. Chem. Acc.* 2008, **120**, 263–271.

88 T. Asada, S. Nagase, K. Nishimoto, S. Koseki, *J. Phys. Chem. B* 2008, **112**, 5718–5727.

89 T. Asada, S. Nagase, K. Nishimoto, S. Koseki, *J. Mol. Liq.* 2009, **147***,* 139–144.

90 T. Asada, S. Hamamura, T. Matsushita, S. Koseki, *Res. Chem. Intermediates*, 2009, **35**, 851–863.

91 S. Koseki, T. Asada, T. Matsushita, *J. Comput. Theoret. Nanoscience*, 2009, **6**, 1352–1360.

92 T. Asada, K. Ohta, T. Matsushita, S. Koseki, *Theoret. Chem. Acc.* 2011, **130**, 439–448.

Table Captions

Table 1. Energy differences (kcal/mol) among geometrical isomers.

Table 2. Spectral peak wavelengths (nm) and transition dipole moments (TDM) $(e \cdot bohr)$ of phosphorescence in iridium complexes.

Table 3. Bond angles (degree) and their sums in NH_2 and NO_2 substituents and the dihedral angles (degree) between the substituents and the phenyl rings of ppy ligands at the geometries optimized for the lowest triplet states.

Figure Captions

Figure 1. Substitution sites in *fac*-Ir(ppy)$_3$.

Figure 2. Emission spectra calculated by the MCSCF+SOCI+SOC method. Each spectral line was calculated as the superposition of Lorentz functions centered at the electronic transition energies from excited spin-mixed (SM) states to the ground state, where a temperature of 400 K was assumed for the thermal distribution of excited SM states, because of overestimating the transition energies, and a half-value width of 6 cm^{-1} was used for all Lorentz functions. (a) Ir(Fppy)$_3$, (b) Ir(NH_2ppy)$_3$, (c) Ir(NO_2ppy)$_3$, and (d) Ir(CNppy)$_3$.

Figure 3. HOMO and LUMO in the parent molecule, *fac*-Ir(ppy)$_3$, where the value of equi-surface is 0.02 $e/bohr^3$.

Figure 4. Orbital interaction between a ppy ligand and a substituent in *facial* (*fac*) isomers. (a) Z = F or NH_2. (b) Z = NO_2 or CN.

Figure 5. Numbering of atoms. X and X' indicate H or O (see **Table 3**).

Figure 6. Geometrical structures of *fac*-Ir(NO_2ppy)$_3$. An unexpected bond is formed as indicated by a dotted circle in (a). All NO_2 substituents are located on the π plane of ppy ligands in (b) and (c), while they are displaced from the π plane of ppy ligands as indicated by a dotted circle in (d).

Figure 7. Emission spectra in calculated by the MCSCF+SOCI+SOC method (see the caption of **Figure 2**). NO_2 or CN substituent is introduced to (a) Ir(4,6-dfppy)$_3$ and its derivatives, (b) Ir(3,4,6-tfppy)$_3$ and its derivatives, and (c) Ir(4,6-dappy)$_3$ and its derivatives, where Ir(5-NO_2-4,6-dappy)$_3$ has very small intensity.

Figure 8. Geometrical structures of *fac*-Ir(5-NO_2-4,6-dfppy)$_3$. All NO_2 substituents are displaced from the π plane of ppy ligands.

2015/04/13

Table 1. Energy differences (kcal/mol) among geometrical isomers.

Complex	Isomer	DFT	MCSCF	+SOCI	+SOC	Ref.
$Ir(ppy)_3$	*fac*	0	0	0	0	
$Ir(ppy)_3$	*mer*	6.4	6.1	6.0	5.7	57
$Ir(3\text{-}Fppy)_3$	*fac*	6.5	9.2	10.4	10.0	57
$Ir(4\text{-}Fppy)_3$	*fac*	0	0	0	0	57
$Ir(5\text{-}Fppy)_3$	*fac*	4.9	6.6	6.6	6.5	57
$Ir(6\text{-}Fppy)_3$	*fac*	4.6	5.7	5.9	5.7	57
$Ir(3\text{-}NH_2ppy)_3$	*fac*	9.9	18.5	19.8	18.9	
$Ir(4\text{-}NH_2ppy)_3$	*fac*	0	0	0	0	
$Ir(5\text{-}NH_2ppy)_3$	*fac*	10.8	11.7	12.3	12.1	
$Ir(6\text{-}NH_2ppy)_3$	*fac*	16.3	18.7	19.0	18.8	
$Ir(3\text{-}NO_2ppy)_3$	*fac*	33.1	40.9	40.6	40.2	
$Ir(4\text{-}NO_2ppy)_3$	*fac*	6.5	15.6	11.7	11.8	
$Ir(5\text{-}NO_2ppy)_3$	*fac*	0	0	0	0	
$Ir(6\text{-}NO_2ppy)_3$	*fac*	31.7	44.6	41.5	41.7	
$Ir(3\text{-}CNppy)_3$	*fac*	13.8	18.0	16.3	15.7	
$Ir(4\text{-}CNppy)_3$	*fac*	3.1	7.1	5.7	5.5	
$Ir(5\text{-}CNppy)_3$	*fac*	0	0	0	0	
$Ir(6\text{-}CNppy)_3$	*fac*	8.4	19.4	16.9	16.9	
$Ir(4,6\text{-}dfppy)_3$	*fac*	0	0	0	0	
$Ir(4,6\text{-}dfppy)_3$	*mer*	6.1	5.5	5.5	5.4	
$Ir(3,4,6\text{-}tfppy)_3$	*fac*	0	0	0	0	
$Ir(3,4,6\text{-}tfppy)_3$	*mer*	1.7	0.9	0.7	0.5	

2015/04/13

Table 2. Spectral peak wavelengths (nm) and transition dipole moments (TDM) $(e \cdot bohr)$ of phosphorescence in iridium complexes.

Complex	Isomer	Peak Wavelength (nm)[a]	Principal Contribution[b]	Wavelength (nm)[c]	TDM $(e \cdot bohr)$	TD DFT (nm)[d]	Expt. (nm)[c]	Ref.	$\Delta Q_{S_0-T_1}$ (Å)[e]
$Ir(ppy)_3$	*fac*	491 (0)	SM3 (S_1)	501	0.299	615		57	0.0557
			SM4 (T_1)	491	0.890		510 (298 K)	71	
							515 (RT)	72	
							517 (298 K)	73	
							494 (77 K)	74	
							509 (RT)	75	
	mer	530 (+39)	SM3(T_1)	530	0.255	698		57	0.1611
		511 (+20)	SM4 (S_1)	512	1.156		512 (298 K)	71	
$Ir(3\text{-}Fppy)_3$	*fac*	486 (–5)	SM3 (S_1)	487	0.352	611		57	0.0619
		477 (–14)	SM4 (T_1)	476	0.811				
$Ir(4\text{-}Fppy)_3$	*fac*	456 (–35)	SM3 (S_1)	462	0.233	603		57	0.0413
			SM4 (T_1)	455	0.853				
$Ir(5\text{-}Fppy)_3$	*fac*	517 (+26)	SM3 (T_1)	517	0.328	648		57	0.0520
		504 (+13)	SM4 (T_1)	504	0.888				
$Ir(6\text{-}Fppy)_3$	*fac*	475 (–16)	SM3 (S_1)	483	0.248	594		57	0.0542
			SM4 (T_1)	474	0.874				
$Ir(3\text{-}NH_2ppy)_3$	*fac*	510 (+19)	SM3 (S_1)	510	0.316	790			0.0711
		495 (+4)	SM4 (T_1)	495	0.978				
$Ir(4\text{-}NH_2ppy)_3$	*fac*	442 (–49)	SM4 (T_1)	442	0.934	610			0.0318
$Ir(5\text{-}NH_2ppy)_3$	*fac*	546 (+55)	SM3 (T_1)	546	0.393	791			0.0704
		526 (+35)	SM4 (T_2)	525	0.962				
$Ir(6\text{-}NH_2ppy)_3$	*fac*	482 (–9)	SM4 (T_1)	482	0.974	598			0.0618

2015/04/13

Table 2 (continued)

Complex	Isomer	Peak Wavelength (nm)[a]	Principal Contribution[b]	Wavelength (nm)[c]	TDM $(e \cdot bohr)$	TD DFT (nm)[d]	Expt. (nm)[c]	Ref.	$\Delta Q_{S_0-T_1}$ (Å)[e]
Ir(4-NO_2ppy)$_3$	*fac*	587 (+96)	SM3 (T_1)	587	0.304	747			0.0419
		561 (+70)	SM4 (T_2)	561	0.937				
Ir(5-NO_2ppy)$_3$	*fac*	404 (–87)	SM3 (S_1)	404	0.335	550			0.0425
		396 (–95)	SM4 (T_1)	395	0.972				
Ir(6-NO_2ppy)$_3$	*fac*	650 (+159)	SM3 (T_1)	652	0.280	798			0.0572
		644 (+153)	SM4 (S_1)	643	0.471				
Ir(3-CNppy)$_3$	*fac*	445 (–46)	SM3 (S_1)	449	0.356	636			0.0500
			SM4 (T_1)	442	0.681				
Ir(4-CNppy)$_3$	*fac*	539 (+48)	SM3 (T_1)	539	0.302	676			0.0533
		522 (+31)	SM4 (T_1)	522	0.925				
Ir(5-CNppy)$_3$	*fac*	459 (–32)	SM4 (T_1)	459	0.863	603			0.0403
Ir(6-CNppy)$_3$	*fac*	534 (+43)	SM3 (S_1)	535	0.331	634			0.0621
		521 (+30)	SM4 (T_1)	521	0.869				
Ir(4,6-dfppy)$_3$	*fac*	440 (–51)	SM4 (T_1)	440	0.864	587		57	0.0602
							468 (298 K)	71	
							469 (RT)	75	
Ir(5-NO_2-4,6-dfppy)$_3$	*fac*	374 (–117)	SM2 (T_1)	379	0.158	600			0.0581
			SM3 (S_1)	377	0.349				
			SM4 (T_1)	373	0.735				
Ir(5-CN-4,6-dfppy)$_3$	*fac*	409 (–82)	SM3 (S_1)	414	0.260	585	442 (77 K)	85	0.0453
			SM4 (T_1)	409	0.789				

2015/04/13

Table 2 (continued)

Complex	Isomer	Peak Wavelength (nm)[a]	Principal Contribution[b]	Wavelength (nm)[c]	TDM $(e \cdot bohr)$	TD DFT (nm)[d]	Expt. (nm)[c]	Ref.	$\Delta Q_{S_0-T_1}$ (Å)[e]
$Ir(4,6\text{-dappy})_3$	*fac*	440 (–51)	SM4 (T_1)	440	1.022	592			0.0776
$Ir(5\text{-CN-}4,6\text{-dappy})_3$	*fac*	409 (–82)	SM3 (S_1) SM4 (T_1)	417 409	0.126 0.942	585			0.0882
$Ir(3,4,6\text{-tfppy})_3$	*fac*	435 (–56)	SM4 (T_1)	435	0.808	594	456 (298 K) 486 (298 K)	86 86	0.0480
$Ir(5\text{-}NO_2\text{-}3,4,6\text{-tfppy})_3$	*fac*	418 (–73)	SM4 (S_1)	418	0.095	592			0.0573
$Ir(5\text{-CN-}3,4,6\text{-tfppy})_3$	*fac*	406 (–85)	SM3 (S_1) SM4 (T_1)	409 405	0.278 0.755	595			0.0460

[a]The values in parentheses are the magnitudes of spectral shifts in comparison with that in the corresponding parent complex. The positive or negative value indicates "red shift" or "blue shift".
[b]The main adiabatic component is shown in parenthesis. Note that, even when the main component is singlet, the sum of triplet weights is the largest.
[c]RT = room temperature.
[d]TD DFT wavelengths were calculated at the uDFT geometries optimized for the lowest triplet states, where we picked up the wavelengths of the transition from the lowest triplet (d, π^*) state to the ground state and no spin-orbit couplings were considered.
[e] $\Delta Q_{S_0-T_1}$ is the averaged geometrical displacement of each atom caused by the transition from the lowest triplet state to the ground state (see ref.83).

2015/04/13

Table 3. Bond angles (degree) and their sums in NH_2 and NO_2 substituents and the dihedral angles (degree) between the substituents and the phenyl rings of ppy ligands at the geometries optimized for the lowest triplet states.[a]

Complex	C–N–H	C–N–H	H–N–H	Sum	Dihedral angle	
$Ir(3\text{-}NH_2ppy)_3$	118.6	120.5	120.7	359.8	C_2–C_3–N–H C_2–C_3–N–H’	4.8 179.8
	115.3	115.7	114.2	345.2	C_2–C_3–N–H C_2–C_3–N–H’	17.1 154.0
	112.2	113.3	111.4	337.0	C_2–C_3–N–H C_2–C_3–N–H’	27.2 154.5
$Ir(4\text{-}NH_2ppy)_3$	115.5	116.4	113.4	345.4	C_3–C_4–N–H C_3–C_4–N–H’	21.1 157.9
	113.9	114.5	111.7	340.0	C_3–C_4–N–H C_3–C_4–N–H’	24.1 154.3
	113.7	114.2	111.4	339.3	C_3–C_4–N–H C_3–C_4–N–H’	25.2 154.6
$Ir(5\text{-}NH_2ppy)_3$	118.4	118.4	116.4	353.3	C_4–C_5–N–H C_4–C_5–N–H’	32.8 156.4
	112.3	112.5	109.3	334.2	C_4–C_5–N–H C_4–C_5–N–H’	30.4 154.3
	112.1	112.5	109.2	333.8	C_4–C_5–N–H C_4–C_5–N–H’	17.0 167.2
$Ir(6\text{-}NH_2ppy)_3$	110.2	112.1	108.1	330.4	C_5–C_6–N–H C_5–C_6–N–H’	11.9 132.3
	110.3	111.6	108.2	330.1	C_5–C_6–N–H C_5–C_6–N–H’	12.3 132.6
	110.1	112.0	108.0	330.1	C_5–C_6–N–H C_5–C_6–N–H’	10.0 130.1

2015/04/13

Table 3 (continued)

Complex	C–N–O	C–N–O	O–N–O	Sum		
$Ir(4\text{-}NO_2ppy)_3$	117.7	118.0	124.3	360.0	$C_3–C_4–N–O$ $C_3–C_4–N–O'$	0.5 179.9
	117.7	118.0	124.2	360.0	$C_3–C_4–N–O$ $C_3–C_4–N–O'$	1.9 178.5
	117.7	118.7	123.6	360.0	$C_3–C_4–N–O$ $C_3–C_4–N–O'$	0.1 179.6
$Ir(5\text{-}NO_2ppy)_3$	117.0	118.8	124.2	360.0	$C_4–C_5–N–O$ $C_4–C_5–N–O'$	0.7 179.4
	117.9	118.0	124.1	360.0	$C_4–C_5–N–O$ $C_4–C_5–N–O'$	0.5 179.6
	118.0	118.0	124.0	360.0	$C_4–C_5–N–O$ $C_4–C_5–N–O'$	0.2 179.6
$Ir(6\text{-}NO_2ppy)_3$	117.7	118.0	124.3	360.0	$C_5–C_6–N–O$ $C_5–C_6–N–O'$	50.2 127.6
	117.6	117.7	124.6	359.9	$C_5–C_6–N–O$ $C_5–C_6–N–O'$	64.8 113.4
	120.4	121.2	105.0	346.6	$C_5–C_6–N–O$ $C_5–C_6–N–O'$	19.1 115.8

[a]See **Figure 5**.

2015/03/03

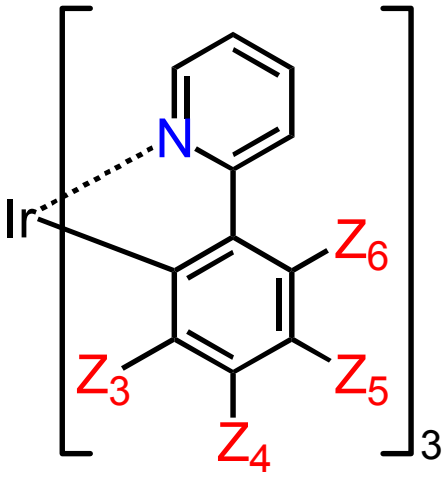

Figure 1 (Koseki *et al.*)

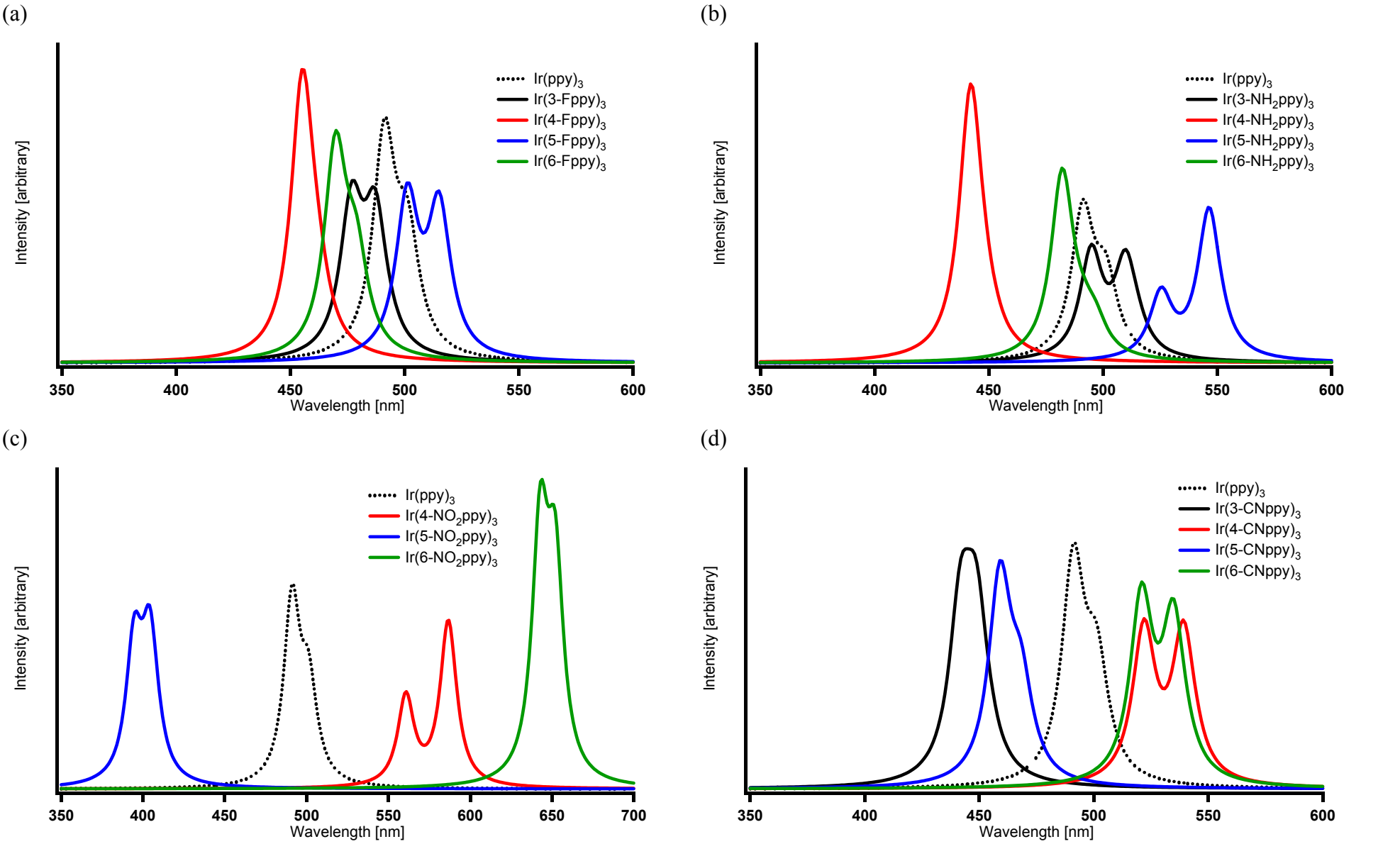

Figure 2 (Koseki *et al.*)

2015/03/03

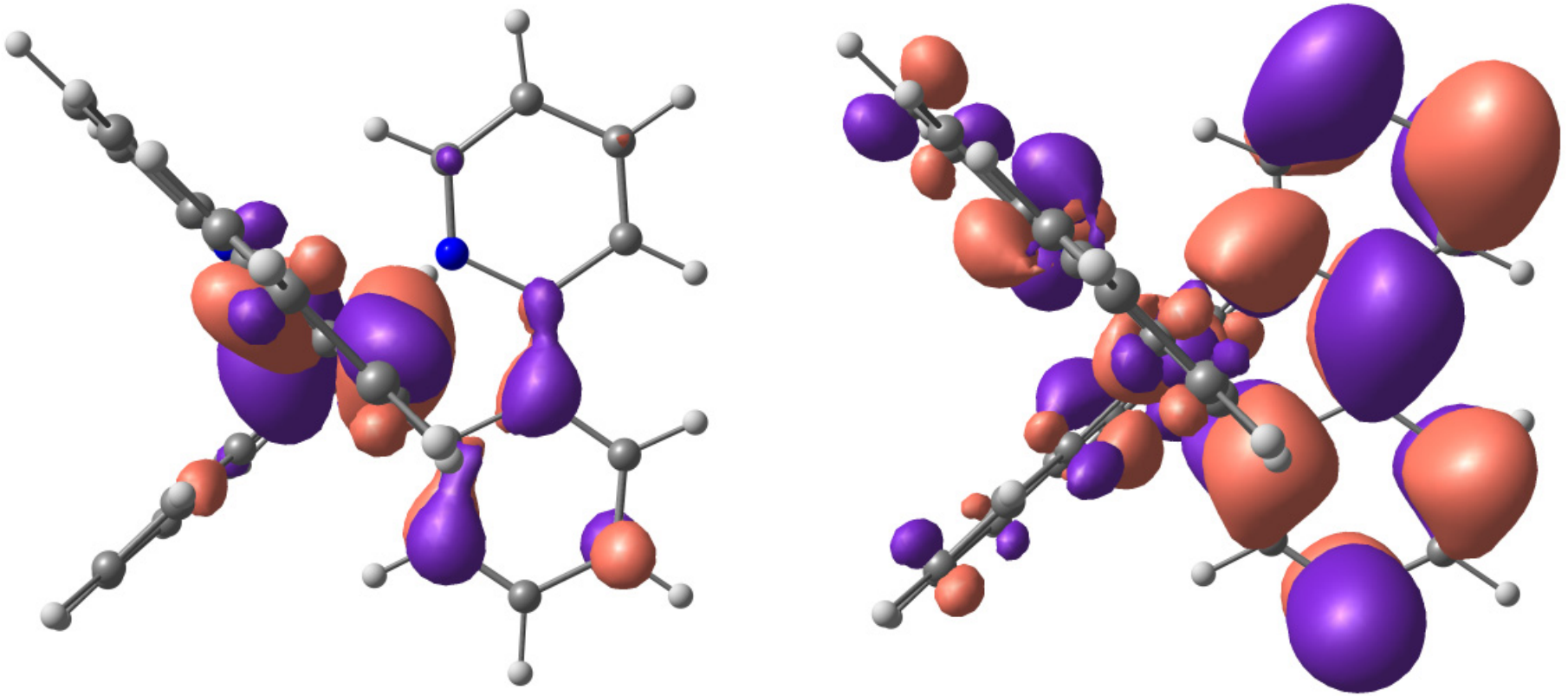

HOMO LUMO

Figure 3 (Koseki *et al.*)

2015/03/03

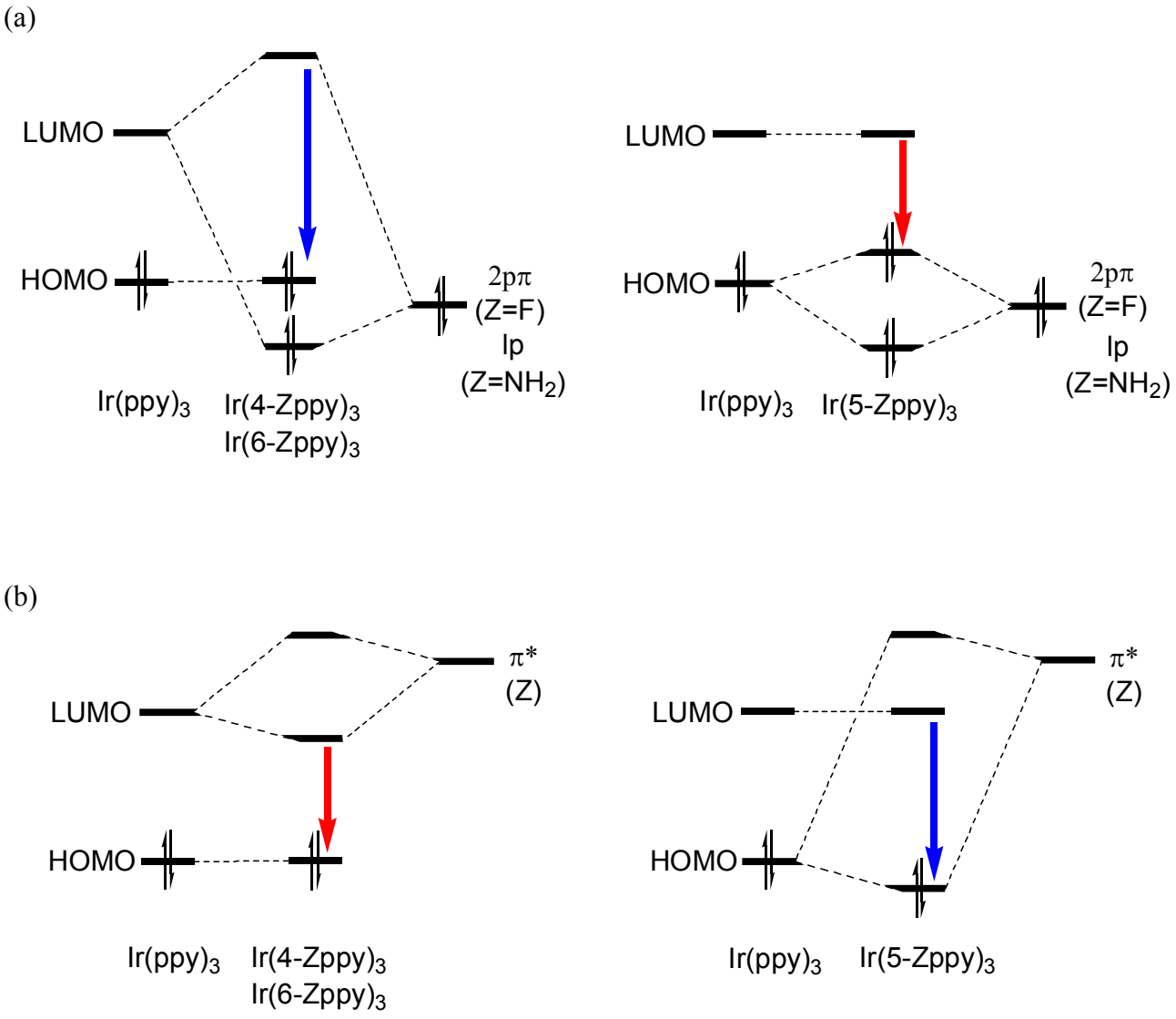

Figure 4 (Koseki *et al.*)

2015/03/03

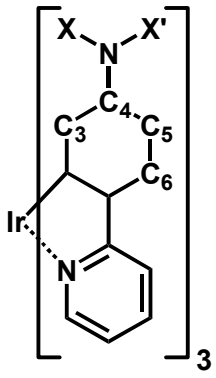

Figure 5 (Koseki *et al.*)

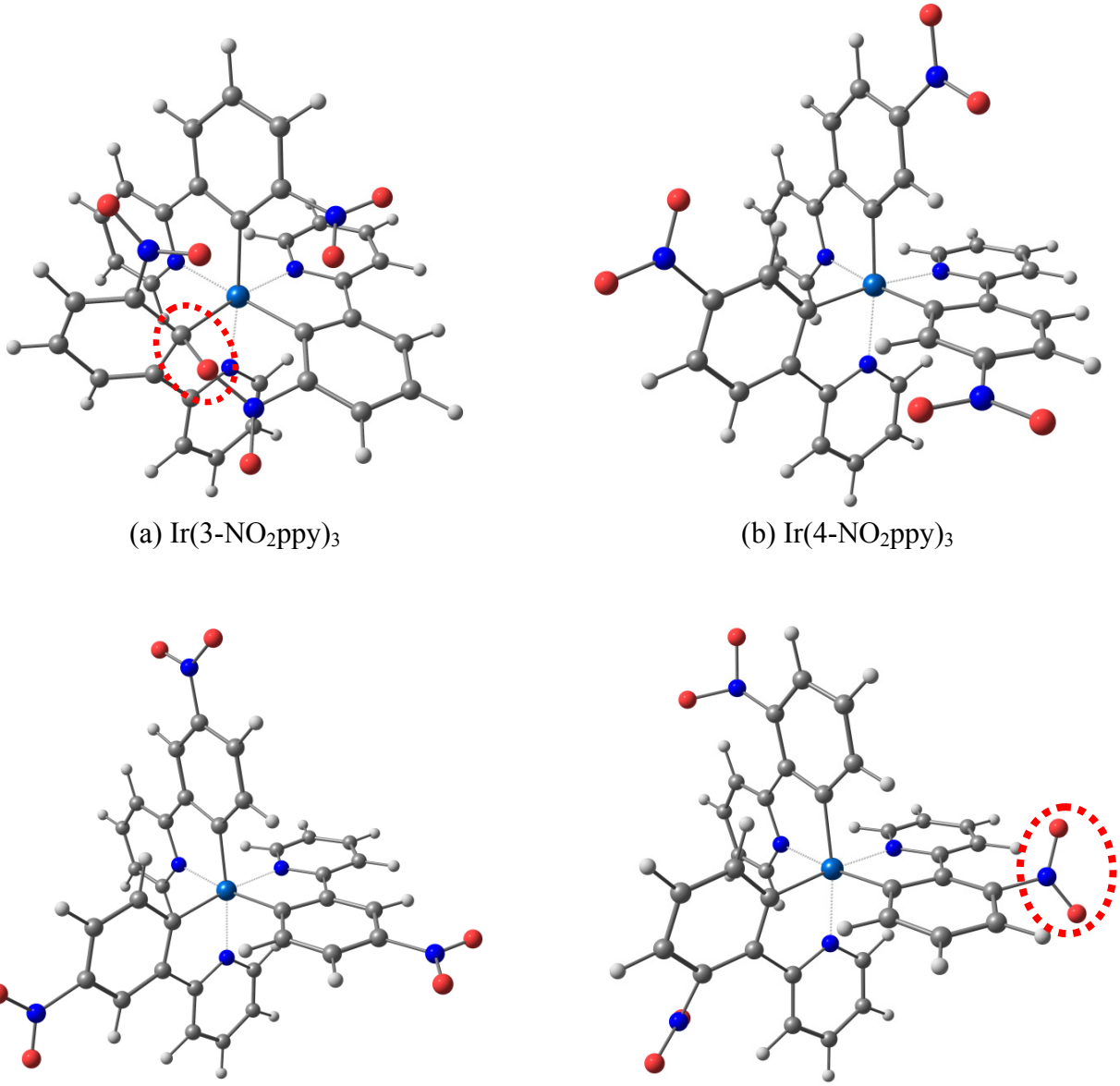

(a) Ir(3-NO_2ppy)$_3$ (b) Ir(4-NO_2ppy)$_3$

(c) Ir(5-NO_2ppy)$_3$ (d) Ir(6-NO_2ppy)$_3$

Figure 6 (Koseki *et al.*)

2015/03/03

(a)

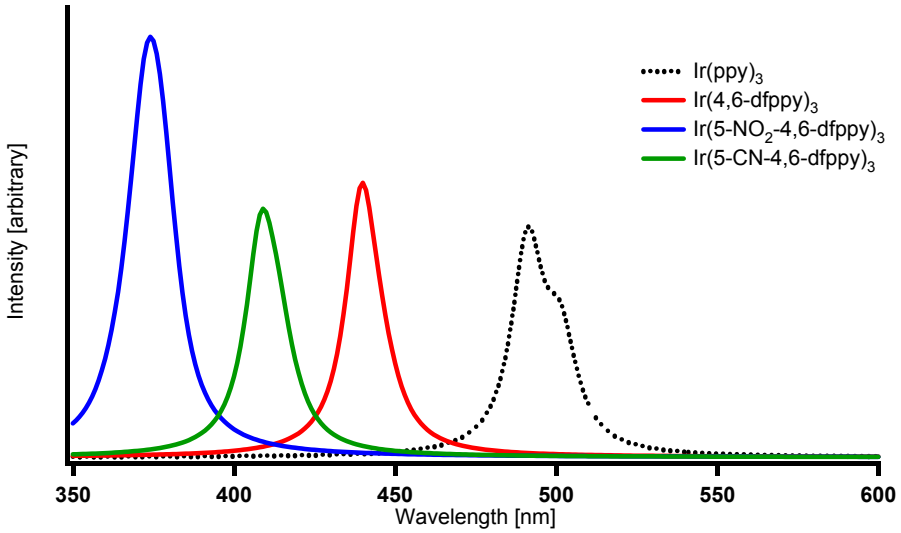

(b)

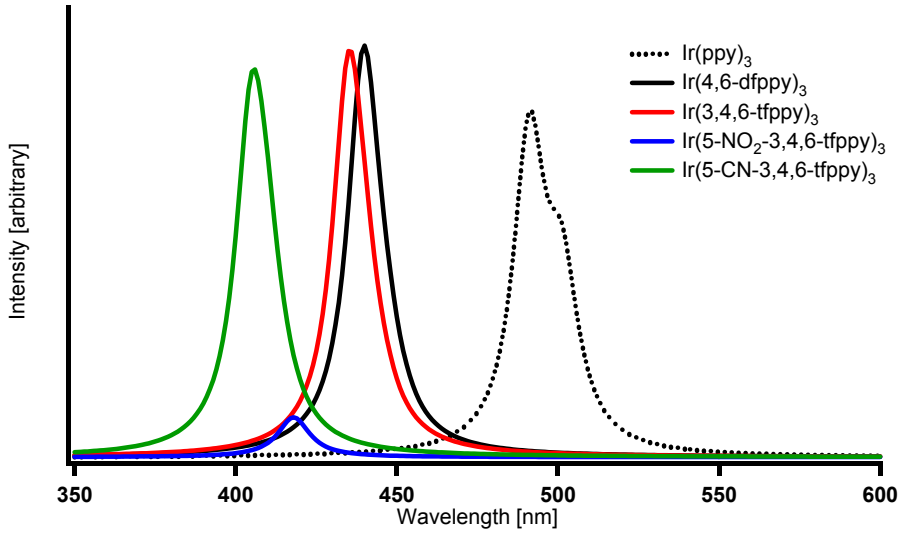

(c)

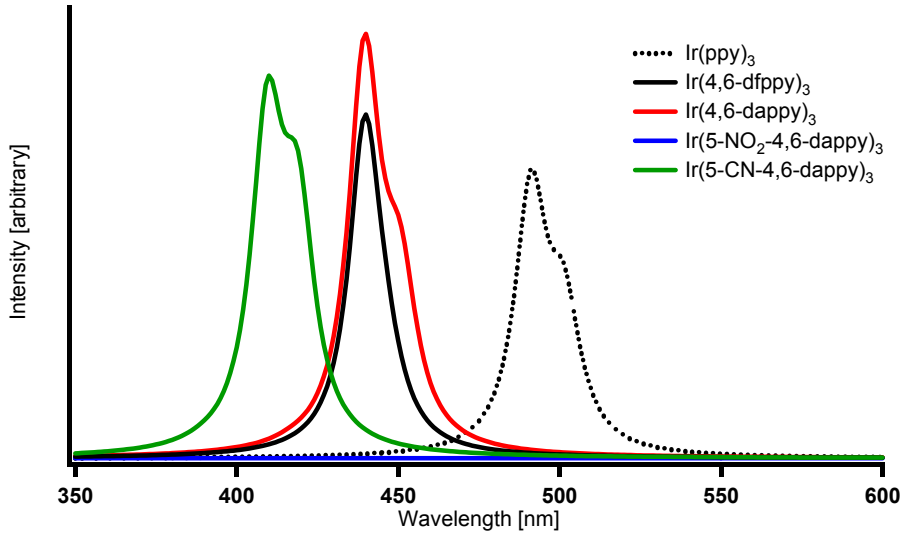

Figure 7 (Koseki *et al.*)

2015/03/03

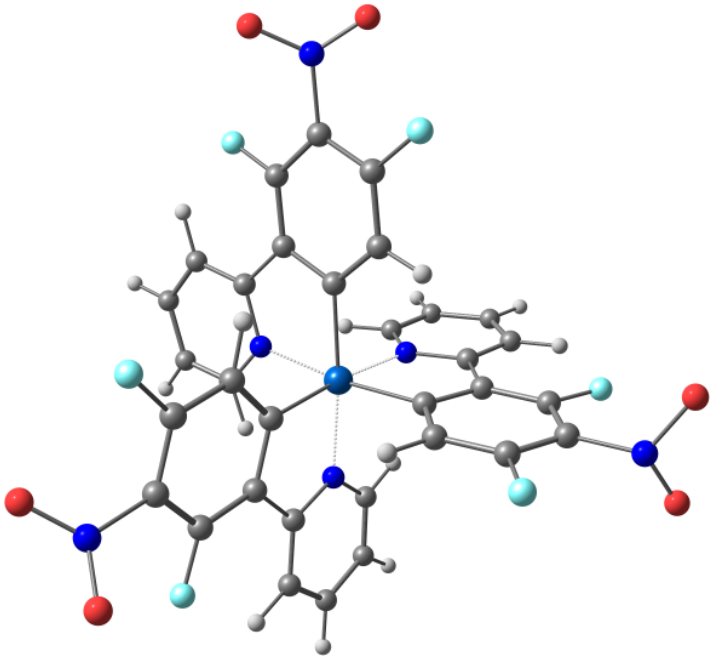

Figure 8 (Koseki *et al.*)